GEOPHYSICS, VOL. 61, NO. 5 (SEPTEMBER-OCTOBER 1996); P. 1301–1307, 5 FIGS.

Some refinements on the finite-difference method for 3-D dc resistivity modeling

Shengkai Zhao* and Matthew J. Yedlin‡

ABSTRACT

Two basic refinements of the finite-difference method for 3-D dc resistivity modeling are presented. The first is a more accurate formula for the source singularity removal. The second is the analytic computation of the source terms that arise from the decomposition of the potential into the primary potential because of the source current and the secondary potential caused by changes in the electrical conductivity. Three examples are presented: a simple two-layered model, a vertical contact, and a buried sphere. Both accurate and approximate Dirichlet boundary conditions are used to compute the secondary potential. Numerical results show that for all three models, the average percentage error of the apparent resistivity obtained by the modified finite-difference method with accurate boundary conditions is less than 0.5%. For the vertical contact and the buried sphere models, the error caused by the approximate boundary condition is less than 0.01%.

INTRODUCTION

In dc resistivity modeling, there are three principal numerical techniques that exist in the literature: integral equation approaches, finite-element methods, and finite-difference methods. Each technique has its own particular advantage and is suitable for particular model geometries.

The integral equation method (Lee, 1975) is based on the accessibility of a known Green's function for a background model. This Green's function is substituted into an integral equation for the potential of an anomalous body inserted into the background model. The integral equation is solved recursively, resulting in a Neumann series. With this technique, Lee (1975) computed the potential of a cylinder or sphere in a layered earth, and Xu et al. (1988) computed 3-D terrain effects for dc resistivity surveys. Since a Green's function is used explicitly, the source singularity is included automatically and does not require special treatment.

The finite-element method is particularly suitable for models with complex geometries, especially in three dimensions. Coggon (1971) derived an energy functional for 2-D electromagnetic problems, including dc resistivity. Using a trial solution based on linear interpolation defined on triangles, he obtained a linear system of equations for the interpolation weights. Pridmore et al. (1981) extended this method to 3-D problems using tetrahedral elements and compared their solution to the integral equation method. Holcombe and Jiracek (1984) used distorted elements to accommodate 3-D topographic variations. The boundary conditions were implemented using approximate analytic boundary conditions that model the potential in a horizontally layered earth. The near-surface layers of regular hexahedral elements were replaced with contiguous distorted isoparametric elements. This distortion was accomplished via coordinate transformation introduced into the finite-element functional.

Finite-difference resistivity modeling for arbitrary 2-D structures was developed in Mufti (1976). He used a nonuniform grid and obtained a self-adjoint system of difference equations after application of a central-difference approximation. This system was efficiently solved using a successive line over relaxation technique. Dey and Morrison (1979) developed a 3-D finite-difference method to evaluate the potential about a point source of current. The generalized Poisson's equation, which includes a spatially variable electrical conductivity, was integrated over elemental volumes to obtain a system of self-adjoint difference equations. An absorbing boundary condition was introduced, based on the asymptotic behavior of the potential at large distances from the source or any material inhomogeneity. The potential was computed for 3-D block-shaped models, including a basin and range geothermal model. James (1985) presented an alternative to the conventional 3-D finite-difference method. He introduced a class of matrix transforms, known as the Polozhii transforms, which are

Manuscript received by the Editor October 25, 1993; revised manuscript received November 21, 1995.
*Formerly Department of Geophysics and Astronomy, University of British Columbia, Vancouver, B.C. Canada V6T 1Z4; presently Western Atlas International Inc., 10205 Westheimer Rd., Houston, Texas 77042.
‡Department of Geophysics and Astronomy, University of British Columbia, Vancouver, B.C., Canada V6T 1Z4.

a generalization of potential-field continuation operators. By decomposing an arbitrary 3-D structure into blocks with arbitrary 1-D property variation, and applying the Polozhii transforms, he obtained a very efficient finite-difference modeling algorithm.

In this paper, we present a combination of two modifications to the finite-difference method for 3-D dc resistivity problem. The first is a more accurate formula for the singularity removal as suggested in Lowry et al. (1989). He showed that removing the source singularity by splitting the potential into primary and secondary potentials improved accuracy since a major proportion (40% or more for the models considered) of the numerical error arose because of the inadequate representation of the source on a discrete grid. A consequence of the introduction of this primary potential into the 3-D dc resistivity problem was the creation of an additional effective source term. The analytic evaluation of the volume integral of this term comprises the second modification. The computation of the secondary potential employs a no-flow boundary condition on the air-earth interface and Dirichlet conditions for the other boundaries.

To test these refinements, three examples were used: a simple two-layered model, a vertical contact, and a buried sphere. In all three cases, analytic solutions were available for comparison. For each case, the analytic solution was compared to the modified finite-difference solution that was implemented using exact analytic boundary conditions and the approximate homogeneous boundary conditions for the secondary potential. For the buried sphere and the vertical contact, the average percentage error was less than 0.25%. For the two-layered model the average percentage error was 65.59% for the approximate boundary conditions and 0.42% for the analytic boundary conditions.

THE MODIFIED BOUNDARY VALUE PROBLEM AND SINGULARITY REMOVAL

Without losing any generality, we assume the source current is located at the origin, since any other point can be easily converted to the origin by a coordinate translation. The fundamental task for forward dc resistivity modeling is to solve the boundary value problem:

$$\nabla \cdot (\sigma \nabla u) = -I\delta(x, y, z) \quad \text{in } \Omega, \text{ the computational domain,} \tag{1a}$$

$$\frac{\partial u}{\partial n} = 0 \quad \text{on the ground surface, and} \tag{1b}$$

$$\frac{\partial u}{\partial n} + \frac{\cos\theta}{r} u = 0 \quad \text{on the other boundaries,} \tag{1c}$$

where the conductivity $\sigma(x, y, z)$ is a known function, u is the potential to be solved, I is the source current, (x, y, z) is the Cartesian coordinate of a point in Ω and θ the angle between the outward unit normal to the boundary, $\hat{\mathbf{n}}$ and the unit radial vector, $\hat{\mathbf{r}}$. The homogeneous, no-flow, Neumann boundary condition equation (1b) is prescribed on the ground surface because no current crosses it. The other external boundary conditions (except for the air-earth surface) are given by the mixed condition as discussed in Dey and Morrison (1979). These are approximate boundary conditions obtained using the assumption that the potential u, far from any inhomogeneity, is of the asymptotic form $1/r$. This mixed condition is obtained by eliminating the explicit dependence of the potential on the conductivity.

At the source point, the potential is singular. If we solve u directly using equation (1), the singularity will cause a large error. A better approach is to remove the effect of the primary, singular potential caused by the source. This can be done in a number of different ways. Coggon (1971), employing a finite-element method, introduced the current source directly into the energy functional, effectively smoothing the source singularity over the neighboring triangular elements. Charbeneau and Street (1979) separated their solution for the hydraulic head in a groundwater flow problem into two parts, a Green's function G to represent the effect of an injection well and a smoother function h that could be modeled by a weighted sum of finite-element basis functions. An application of the Galerkin principle resulted in a modified system of linear equations with new effective sources caused by the inclusion of the source function G. Lowry et al. (1989) employed a similar method for removing the source singularity by splitting the potential into the primary potential ϕ caused by the current source in a uniform half-space and the secondary potential ψ caused by the conductive inhomogeneities. Thus,

$$u = \phi + \psi. \tag{2}$$

However, Lowry et al. gave the primary potential as

$$\phi = \frac{I}{2\pi\bar{\sigma}\sqrt{x^2 + y^2 + z^2}}, \tag{3}$$

where $\bar{\sigma}$ was defined as the average conductivity of the whole domain. With the above formula, the singularity cannot be removed completely in the neighborhood of the source point where the singularity effects are the greatest. It appears that both Li (1992) and McGillivray (1992) noticed this problem. The more accurate formula is

$$\phi = \frac{I}{2\pi\sigma_0\sqrt{x^2 + y^2 + z^2}}, \tag{4}$$

if the source point is on the ground surface, or

$$\phi = \frac{1}{4\pi\sigma_0\sqrt{x^2 + y^2 + z^2}}, \tag{5}$$

if the source is underground, where σ_0 is the conductivity of the media at the source point.

In this paper, we will assume that the source point is on the ground surface and take equation (4) as the primary potential field. Substituting equation (2) into equation (1a) yields

$$\nabla \cdot (\sigma \nabla \psi) = -[I\delta(x, y, z) + \nabla \cdot (\sigma \nabla \phi)] \quad \text{in} \quad \Omega, \text{ the computational domain.} \tag{6}$$

We note the appearance of a new effective source term on the right-hand side, a consequence of the introduction of the primary field ϕ caused by the source. Since no current crosses the ground surface, the boundary condition for ψ on the ground

surface is given by

$$\frac{\partial \psi}{\partial n} = 0. \tag{7}$$

It remains to set the boundary condition for ψ on the other boundaries. The condition of Dey and Morrison (1979) is a direct consequence of the far-field asymptotic form of the solution for the potential u. However, the far-field asymptotic form for ψ cannot be determined readily a priori. For example, if the secondary potential ψ is dipolar and of the form of a vertical dipole,

$$\psi = \frac{\cos\theta}{r^2}, \tag{8}$$

then the mixed boundary condition should be

$$\frac{\partial \psi}{\partial n} + \frac{\sin\theta}{r}\psi = 0. \tag{9}$$

Note that the form of equation (9) is different from equation (1c) with the sine replacing the cosine term. Since, in general, it is not possible to know the asymptotic form for the secondary potential, we use the robust choice that

$$\psi = 0 \tag{10}$$

on the other boundaries. This choice is based on the fact that for most models, if the boundaries are far from the inhomogeneity, the secondary potential will go to zero at least as fast as $1/r^2$.

THE FINITE-DIFFERENCE METHOD

Now we solve the boundary value problem consisting of equations (6), (7), and (10) by the finite-difference method. We divide domain Ω into $N_x N_y N_z$ rectangular cells (see Figure 1) with dividing planes $x = x_i\,(i = 1, \ldots, N_x + 1, y = y_j\,(j = 1, \ldots, N_y + 1)$, and $z = z_k\,(k = 1, \ldots, N_z + 1)$. The boundary planes of Ω correspond to $i = 1$ or $N_x + 1$, $j = 1$ or $N_y + 1$ and $k = 1$ or $N_z + 1$. All other index values correspond to interior points. The nodal intervals are $\Delta x_i = x_{i+1} - x_i$, $\Delta y_j = y_{j+1} - y_j$ and $\Delta z_k = z_{k+1} - z_k$. In each cell, the conductivity is approximated by a constant that is chosen as the conductivity at the center of the cell. In this paper, a grid point (x_i, y_j, z_k) will be represented by (i, j, k). The cell with diagonal points (i, j, k) and $(i+1, j+1, k+1)$ has a conductivity $\sigma_{i,j,k}$.

At any interior grid point (i, j, k), we define a rectangular prism, $V_{i,j,k} = \{(x, y, z) | (x_{i-1} + x_i)/2 \le x \le (x_i + x_{i+1})/2, (y_{j-1} + y_j)/2 \le y \le (y_j + y_{j+1})/2, (z_{k-1} + z_k)/2 \le z \le (z_k + z_{k+1})/2\}$ (see Figure 2). The enclosure of $V_{i,j,k}$ is denoted by $S_{i,j,k}$. We integrate both sides of equation (6) over the elemental volume $V_{i,j,k}$ to obtain

$$\int_{V_{i,j,k}} \nabla \cdot (\sigma \nabla \psi) dv = -\int_{V_{i,j,k}} [I\delta(x, y, z) + \nabla \cdot (\sigma \nabla \phi)] dv. \tag{11}$$

Using Gauss's theorem, from equation (11) we obtain

$$\oint_{S_{i,j,k}} (\sigma \nabla \psi) \cdot ds = -\int_{V_{i,j,k}} [I\delta(x, y, z) + \nabla \cdot (\sigma \nabla \phi)] dv. \tag{12}$$

The discretization of the left-hand side of equation (12) and the derivation of the coefficient matrix are the same as that presented in Dey and Morrison (1979) and will be omitted for brevity. The only difference is that we don't need to build equations for those boundary points where the values of ψ are given by the homogeneous Dirichlet boundary condition.

Now we present the analytic formulation to compute the right-hand side of equation (12). Lowry et al. computed this term numerically [Lowry et al., 1989, 770, equation (15)]. We denote the right-hand side of equation (12) by $f_{i,j,k}$. Then we have

$$f_{i,j,k} = -\int_{V_{i,j,k}} [I\delta(x, y, z) + \nabla \cdot (\sigma \nabla \phi)] dv. \tag{13}$$

At the source point, assuming σ is constant, $f_{i,j,k}$ is identically equal to zero. This can be seen by expanding the second term on the right-hand side of equation (13). At all other points, which are source-free, the first term on the right-hand side of equation (13) yields zero. Therefore,

$$f_{i,j,k} = -\int_{V_{i,j,k}} \nabla \cdot (\sigma \nabla \phi) dv. \tag{14}$$

In a volume where the conductivity is constant, because $\nabla \cdot (\sigma \nabla \phi) = \sigma \nabla^2 \phi = 0$, the integral on the right-hand side of equation (14) is zero. In a volume containing a discontinuity of conductivity, the integration is not zero. From Figure 2, we note $V_{i,j,k}$ contains one-eighth of each of the eight cells that are common to the central point (i, j, k). Each cell can have different conductivity. There are a total of 12 interfaces between these cells. We have to consider them separately. As an example, let us consider the integration over a small volume

$$V_\epsilon = \{(x, y, z) | x_i - \epsilon \le x \le x_i + \epsilon, \quad y_j \le y \le (y_j + y_{j+1})/2, (z_{k-1} + z_k)/2 \le z \le z_k\},$$

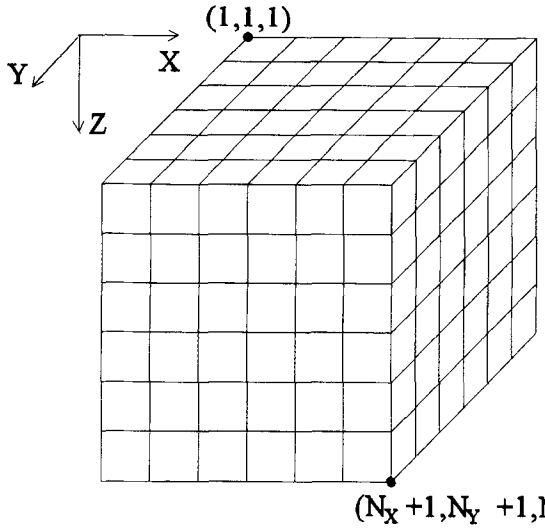

FIG. 1. The 3-D finite-difference grid. The nodes are numbered from (1, 1, 1) to $(N_x + 1, N_y + 1, N_z + 1)$ as shown in the figure.

which contains the interface $x = x_i$ (see Figure 2, the volume between the two dotted planes),

$$\int_{V_\epsilon} \nabla \cdot (\sigma \nabla \phi) dv = \oint_{S_\epsilon} \sigma \frac{\partial \phi}{\partial n} ds$$

$$= \lim_{\epsilon \to 0} \oint_{S_\epsilon} \sigma \frac{\partial \phi}{\partial n} ds$$

$$= (\sigma_{i,j,k-1} - \sigma_{i-1,j,k-1}) \times \int_{(z_{k-1}+z_k)/2}^{z_k} \int_{y_j}^{(y_j+y_{j+1})/2} \times \frac{\partial \phi}{\partial x} dy\, dz. \quad (15)$$

The integration in equation (15) can be computed analytically. From equation (4), we have

$$\frac{\partial \phi}{\partial x} = -\frac{I}{2\pi\sigma_0} \frac{x}{(x^2 + y^2 + z^2)^{3/2}}. \quad (16)$$

It is easy to verify that

$$\int \frac{x}{(x^2 + y^2 + z^2)^{3/2}} dy\, dz = \tan^{-1} \frac{yz}{x\sqrt{x^2 + y^2 + z^2}}. \quad (17)$$

From equations (15), (16), and (17), we have

$$\int_{V_\epsilon} \nabla \cdot (\sigma \nabla \phi) dv = \frac{I(\sigma_{i-1,j,k-1} - \sigma_{i,j,k-1})}{2\pi\sigma_0} \times \left\{ \tan^{-1} \frac{2(y_j + y_{j+1})z_k}{x_i\left[4x_i^2 + (y_j + y_{j+1})^2 + 4z_k^2\right]^{1/2}} \right.$$

$$- \tan^{-1} \frac{(y_j + y_{j+1})(z_{k-1} + z_k)}{x_i\left[4x_i^2 + (y_j + y_{j+1})^2 + (z_{k-1} + z_k)^2\right]^{1/2}}$$

$$- \tan^{-1} \frac{y_j z_k}{x_i\left[x_i^2 + y_j^2 + z_k^2\right]^{1/2}}$$

$$\left. + \tan^{-1} \frac{2y_j(z_{k-1} + z_k)}{x_i\left[4x_i^2 + 4y_j^2 + (z_{k-1} + z_k)^2\right]^{1/2}} \right\}. \quad (18)$$

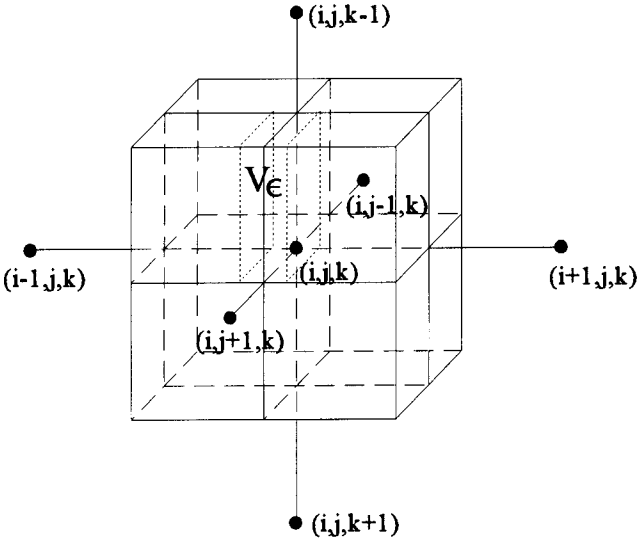

FIG. 2. The rectangular parallelepiped $V_{i,j,k}$ associated with an interior point (i, j, k). There are 8 cells and 12 interfaces within $V_{i,j,k}$. Also shown in this figure is the volume V_ϵ (between the two dotted planes) associated with the surface integral in equation (14).

The integrations on other interfaces can be computed in the same way. For grid points on the ground surface, the same technique is used. There are, however, only four interfaces that need to be considered for each point.

The coefficient matrix is symmetric and sparse. We need to compute and store only the upper half of the coefficient matrix. The resultant equation system is solved by the conjugate gradient method (Kershaw, 1978; Dey and Morrison, 1979; Meijerink and van der Vorst, 1981) with a simple incomplete LDL^T factorization preconditioner.

EXAMPLES

To illustrate the effects of the two modifications to the finite-difference method, in this section we consider the three examples discussed in Lowry et al. (1989): a two-layered model, a vertical contact, and a buried sphere. Analytical solutions are available for all three models. We use the analytic solution for comparison and also for the accurate boundary conditions in finite-difference computations. In practice, usually we do not have the luxury of having an analytic solution. In that situation, we can approximate the boundary condition for the secondary potential by equation (10). It is equivalent to setting the total potential to the primary potential. This choice is based on the fact that the secondary potential is caused by the charge distribution result of the changes in conductivity. For most models, if the boundaries are far from the inhomogeneity, the secondary potential is mainly a dipole field and will go to zero at least as fast as $1/r^2$. The computation of the apparent resistivity from the known potential is quite straightforward, which can be found from the papers by either Lowry et al. (1989) or Dey and Morrison (1979). In the following, for each case, we will compute the potential by the analytic formula, and the modified finite-difference method, using either the accurate or the approximate homogeneous Dirichlet boundary conditions for the secondary potential. Then we compute the apparent resistivity from those potentials and compare them with the analytical results.

The first example is a dipole-dipole array over a two-layered model shown in Figure 3. The top layer has a conductivity $\sigma_1 = 0.01$ S/m and a thickness $\sigma = 2$ m. The second layer is a uniform half-space with a conductivity $\sigma_2 = 0.1$ S/m. The analytic solution can be obtained from the book written by Keller and Frischknecht (1966, 104–112). The apparent resistivity for this model also is shown in Figure 3. In Figure 3 and in Figures 4 and 5, the open circles o represent the analytic results, the solid triangle ▲ is the result obtained by the modified finite-difference method with accurate boundary conditions, and the plus + is the result obtained by the modified finite-difference method using the approximate Dirichlet condition. It is clear from Figure 3, that the homogeneous Dirichlet boundary condition yields inferior results especially as the boundary of the

computational domain is approached. The average percentage error in this case is 65.69% compared with an average percentage error of 0.42% when the analytic solution is used as the boundary condition. This example unmistakably demonstrates that the use of the homogeneous Dirichlet boundary condition for the secondary potential is valid only when the inhomogeneity is far from the computational boundary. The following models amply verify this intuitive result.

The second example is the Wenner array profiling a vertical contact shown in Figure 4. For this case, the difference between the three calculations of the apparent resistivity is so slight that the o, ▲, and + overlay one another. The average percentage error is 0.23% for the finite-difference solution with accurate boundary conditions and 0.24% for the finite-difference solution with approximate boundary conditions.

The third example is a pole-dipole array profiling over a nonconducting sphere with a conductivity $\sigma_1 = 10^{-8}$ S/m embedded in a half-space with conductivity $\sigma_2 = 0.01$ S/m (Figure 5). The analytic solution was obtained using the code developed in Aldridge and Oldenburg (1989), in which bispherical coordinates were used to solve for the potential. The average percentage error is 0.139% for the finite-difference solution with accurate boundary conditions and 0.143% for the finite-difference solution with approximate boundary conditions, less than the 0.83% obtained by Lowry et al. (1989).

The approximate homogeneous boundary condition worked well for the vertical contact and the sphere, but not for the simple two-layered model, where the conductivity inhomogeneity extended to the boundary. For the cases of the vertical contact and the sphere, the results were excellent. Best results were obtained for the sphere, since it was not near the boundary. The employment of the more accurate source singularity removal and the analytical integration of the source terms, resulted in one-sixth the average relative error obtained by Lowry et al. (1989) who used the source singularity removal combined with mixed boundary conditions.

We can understand the problem from another point of view. In the first example, the secondary potential is a series of point source images on a vertical line that has a form of $1/\sqrt{x^2 + y^2 + (z + na)^2}$. The dominant part $1/\sqrt{x^2 + y^2 + (z + a)^2}$ is quite close to the source point. In this situation, the approximate boundary condition causes large errors in the apparent resistivity. In the second example, the secondary potential is still of the form of $1/x$. However, because of the image factor, the source of the secondary potential is always far away from the boundary. For the third model, the sphere is far from the boundary. The secondary potential is mainly a dipole field, therefore it goes to zero at least as fast a $1/r^2$.

CONCLUSIONS

In this paper, two modifications of the finite-difference method were presented. The first was a more accurate formula for the removal of the source singularity. The second was the analytical evaluation of the right-hand side of the finite-difference equations. These refinements were applied to three models: a simple two-layered model, a vertical contact, and a buried sphere. For these models, both accurate and approximate Dirichlet boundary conditions were used. Numerical results show that with the accurate boundary conditions, the average percentage error of the apparent resistivity obtained by the modified finite-difference method is less 0.5%. The error caused by the approximate homogeneous Dirichlet boundary condition is about 0.01% for the vertical contact and the sphere models, but is much larger for the two-layered model.

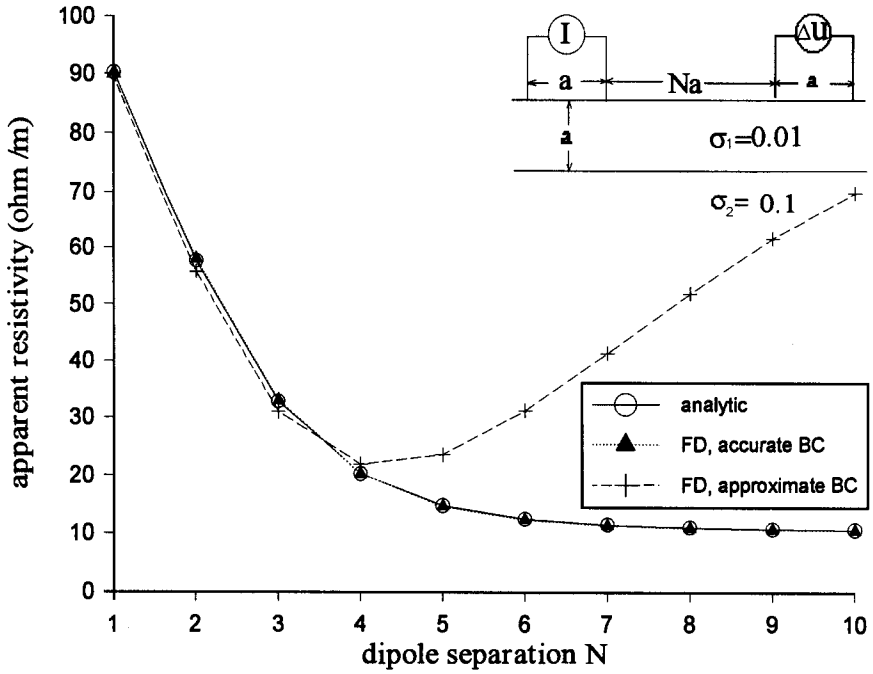

FIG. 3. A dipole-dipole array over a two-layered model. A comparison of the apparent resistivity computation obtained from calculation of the potential using three different methods: analytic solution (o), modified finite difference method using exact boundary condition obtained from the analytic solution, and (▲) and modified finite-difference method using the approximate homogeneous Dirichlet boundary condition for the secondary potential (+).

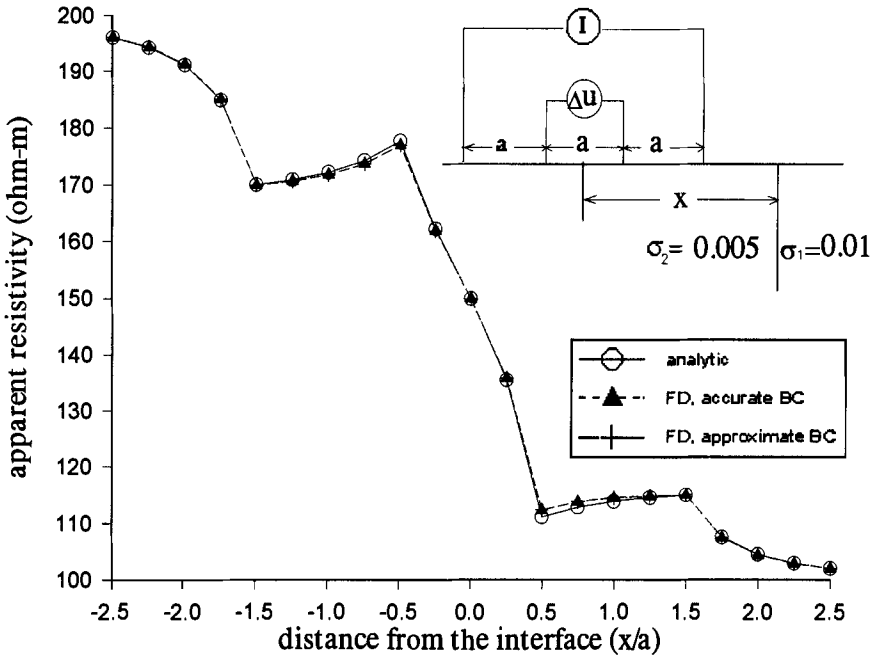

FIG. 4. A Wenner array over a vertical contact. A comparison of the apparent resistivity computation obtained from calculation of the potential using three different methods: analytic solution (o), modified finite-difference method using exact boundary condition obtained from the analytic solution, and (▲) and modified finite-difference method using the approximate homogeneous Dirichlet boundary condition for the secondary potential (+).

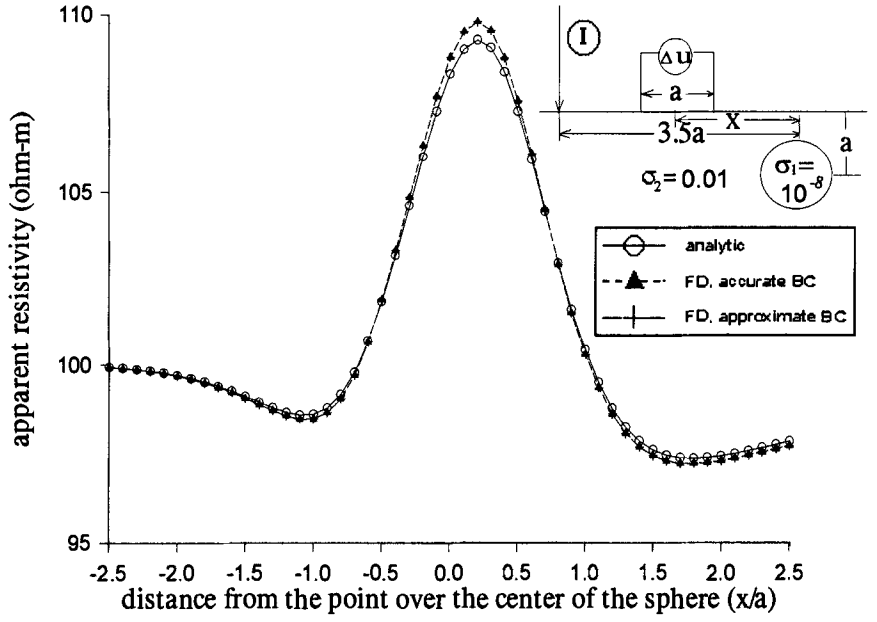

FIG. 5. A polar-dipole array over a nonconducting sphere embedded in a conducting half-space. A comparison of the apparent resistivity computation obtained form calculation of the potential using three different methods: analytic solution (o), modified finite-difference method using exact boundary condition obtained from the analytic solution (▲), and modified finite-difference method using the approximate homogeneous Dirichlet boundary condition for the secondary potential (+).

The results presented suggest a generalization. For models that have analytic solutions, such as a layered medium, the potential may be decomposed into that arising from the layered medium and a secondary potential. The modified finite-difference algorithm presented in this paper could then be employed to handle superimposed localized conductivity anomalies. As demonstrated for the case of the sphere, the homogeneous far-field boundary conditions would obviate the use of the mixed far-field boundary condition.

ACKNOWLEDGMENTS

We wish to thank Professor D. W. Strangway, the president of the University of British Columbia, for providing financial support and many encouragements to S. Zhao during his stay in Univ. of British Columbia. We also wish to thank Dr. Aldridge and Dr. Oldenburg for letting us use their code to compute the analytic solution of the third example in this paper. The comments of the referees greatly improved the original text. This work was supported by Natural Science and Engineering Research Council of Canada (NSERC) operating grant 5-80642 and Professor D. W. Strangway's Univ. of British Columbia research grant.

REFERENCES

Aldridge, D. F., and Oldenburg, D. W., 1989, Direct current electric potential-field associated with two spherical conductors in a whole-space: Geophys. Prosp., **37**, 311–330.

Charbeneau, R. J., and Street, R. L., 1979, Modeling groundwater flow fields containing point singularities; A technique for singularity removal: Water Res. Research, **15**, 583–594.

Coggon, J. H., 1971, Electromagnetic and electrical modeling by the finite-element method: Geophysics, **36**, 132–155.

Dey, A., and Morrison, H. F., 1979, Resistivity modeling for arbitrarily shaped three-dimensional structures: Geophysics, **44**, 753–780.

Holcombe, H. T., and Jiracek, G. R., 1984, Three-dimensional terrain corrections in resistivity surveys: Geophysics, **49**, 439–452.

James, B. A., 1985, Efficient microcomputer-based finite difference resistivity modeling via Polozhii decomposition: Geophysics, **50**, 443–465.

Keller, G. V., and Frischknecht, F. C., 1966, Electrical methods in geophysical prospecting: Pergamon Press, Inc.

Kershaw, D. S., 1978, The incomplete Cholesky-conjugate gradient method for the iterative solution of systems of linear equations: J. Comput. Phys., **26**, 43–65.

Lee, T., 1975, An integal equation and its solution for some two and three-dimensional problems in resistivity and induced polarization: Geophys. J., **42**, 81–95.

Li, Y., 1992, Inversion of three-dimensional direct current resistivity data: Ph.D. thesis, Univ. of British Columbia.

Lowry, T., Allen, M. B., and Shive, P. N., 1989, Singularity removal: A refinement of resistivity modeling techniques: Geophysics, **54**, 766–774.

McGillivray, P. R., 1992, Forward modeling and inversion of dc resistivity and MMR data: Ph.D. thesis, Univ. of British Columbia.

Meijerink, J. A., and van der Vorst, H. A., 1981, Guidelines for the usage of incomplete decompositions in solving sets of linear equations as they occur in practical problems: J. Comput. Phys., **44**, 134–155.

Mufti, I. R., 1976, Finite-difference resistivity modeling for arbitrarily shaped two-dimensional structures: Geophysics, **41**, 62–78.

Pridmore, D. F., Hohmann, G. W., Ward, S. H., and Sill, W. R., 1981, An investigation of finite-element modeling for electrical and electromagnetic data in three dimensions: Geophysics, **46**, 1009–1024.

Xu, S. Z., Gao, Z. C., and Zhao, S. K., 1988, An integral formulation for three-dimensional terrain modeling for resistivity surveys, Geophysics, **53**, 546–552.